Received: 25 September 2018 | Revised: 20 March 2019 | Accepted: 20 March 2019

DOI: 10.1002/rnc.4553

RESEARCH ARTICLE

WILEY

Robust plant by plant control design using model-error tracking sets

Arnold Pretorius | Edward Boje

Department of Electrical Engineering, University of Cape Town, Cape Town, South Africa

Correspondence
Arnold Pretorius, Department of Electrical Engineering, University of Cape Town, Cape Town 7701, South Africa.
Email: prtarn001@myuct.ac.za

Funding information
South African National Research Foundation, Grant/Award Number: 115244

Summary

This paper presents a method for designing a robust two-degree-of-freedom control scheme, capable of satisfying multiple model-error specifications on a plant by plant basis. Traditional quantitative feedback theory methods generally use a single model-error or above-below magnitude tracking specification, which can result in overdesign for plants located away from the bounding conditions. The performance specifications are also generally hand-tuned, or iteratively adjusted to keep the underlying time-domain signals within permissible levels. Our method aims to perform a model-error design on a per-plant basis, such that each plant's corresponding model tracking has equal weighting given the plant's inherent feedback requirements and capability. The quantitative feedback theory method allows this per-plant approach to be undertaken with ease. Additionally, sufficiently low-order model specifications are designed using simple optimisation, which take into account performance limiting effects, such as non-minimum phase behaviour and signal constraints. A worked example is presented, showing the viability and transparency of the proposed method.

KEYWORDS

QFT, robust control, tracking error specifications

1 | INTRODUCTION

Linear robust feedback control problems are generally cast in the frequency-domain, and take the form of two-degree-of-freedom (2DOF) controllers.[1] The bandwidth trade-off between the two controller elements, conventionally being the prefilter and feedback controller, as shown in Figure 1, is not however obvious. Most commonly employed among quantitative feedback theory practitioners is the method of magnitude-based tracking bounds.[2-4] In this form, one can specify per-frequency above and below magnitude bounds on the closed-loop system. This method inherently facilitates the trade-off between the prefilter and feedback controller. There is however no explicit specification on the closed-loop phase requirement, which can lead to over/underdesign of the controller and degradation of the tracking precision.[5] This can be remedied by adding above and below phase constraints to the closed-loop system.[6] This will generate a second set of per-frequency bounds, whereby the global solution space is the intersection of the magnitude and phase-derived bounds. Model-error tracking specifications, also known as model matching, use the magnitude of the closed-loop tracking error, thereby including phase information in the solution space.[7] In this context, one method of

Arnold Pretorius and Edward Boje contributed equally to this work.

Abbreviations: 2DOF, two-degree-of-freedom; QFT, quantitative feedback theory; NMP, non-minimum phase.

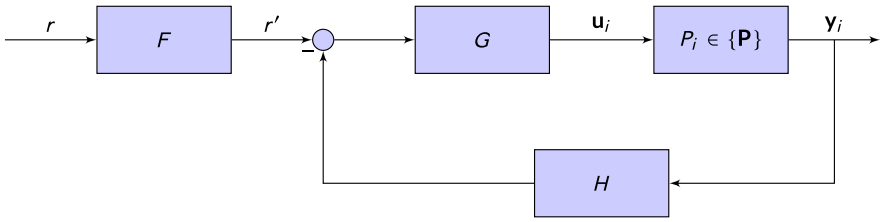

FIGURE 1 Block diagram of standard control scheme with two degrees of freedom [Colour figure can be viewed at wileyonlinelibrary.com]

resolving the 2DOF trade-off is to fix the prefilter based on the model and closed-loop nominal plant inverse, prior to the feedback design. Depending on the extent and variety of the plant uncertainty, the choice of nominal plant may introduce conservatism into the bound generation of the feedback controller.[8] Additionally, the order of this prefilter can be impractically high. Boje[9] solved this by redesigning the prefilter, using closed-loop tracking error specifications, after the feedback controller has been fixed. More recent work done by Elso et al[8,10] outlined two methods of designing the prefilter and feedback controller in a model-error form, with no dependence of the nominal plant choice. Elso et al[10] developed an inequality solely dependent on the feedback control element, which, if satisfied, guarantees the existence of a non-empty solution space to the prefilter, based on the standard model-error tracking inequality. This effectively decouples the design of the feedback controller and prefilter, allowing them to be designed sequentially, without any conservatism imposed on the generated bounds. The aforementioned methods only use a single tracking specification for all plant conditions, meaning that a valid solution unavoidably leads to over/underdesign of certain plants, which do not sit close to the boundary conditions.

In practice, proper control design requires realistic performance specifications, which reflects the plants limitations, be it non-minimum phase (NMP) behaviour or input constraints. These specifications are generally treated as "client given" or "tuned" until the specifications are achievable. As the specifications do not directly take time-domain signal limits into account, finding a valid solution may yield unacceptable plant signals (eg, input-rate saturations), which can degrade performance, and potentially lead to instability. Franchek and Herman[11] developed gain-phase constraints on the open-loop system, to ensure that the closed-loop plant input of a one-degree-of-freedom system does not saturate in amplitude, when being excited by a step input of constrained magnitude. Horowitz[12] and Wu and Jayasuriya[13] avoided signal saturations by embedding a controlled artificial saturation block in front of the actual saturation block. A cascaded internal feedback structure is then designed such that when the artificial element saturates, the system is still closed-loop stable. This has the effect of nonlinearly reducing the closed-loop bandwidth as the signal magnitude increases. Pritchard and Wigdorowitz[14] chose above-below tracking bounds to ensure that the worst-case plant (in terms of gain and phase) cannot saturate within the valid design space. Although this does constrain the plant input signal, it imposes conservatism over the entire plant set, especially high gain cases. Other research on the input saturation problem exists, with respect to the quantitative feedback theory design framework.[15]

The work presented in this paper resolves the aforementioned design shortfalls. First, a sufficiently low-order model set, which realistically reflects the associated plant set capabilities, is found via simple optimisation. A per-plant model-error inequality is then developed, based on the work of Elso et al,[10] which is used to find the local solution space of the feedback controller. A global controller solution space (across all plants) is then generated by finding the intersection across all local solution spaces. An appropriate feedback controller can then be designed to lie in each discrete design frequency-based solution space. Once the feedback controller has been fixed, the prefilter is designed by applying the original model-error specifications to the closed-loop transfer behaviour. Both elements are designed using a level set of error radii, which gives transparency in the discrete frequency to frequency performance trade-offs. The effectiveness of this method is demonstrated with an example in Section 3.

2 | PROPOSED METHOD

2.1 | Problem statement

Given a known, ordered plant set $P_i \in \{\mathbf{P}\}, i = \{1, 2, \ldots, m\}$, a corresponding ordered set of closed-loop tracking models $M_i \in \{\mathbf{M}\}$ can be specified/designed based on the plant capabilities and signal levels. Plant P_i may be unstable and/or NMP, and may have time-domain input constraints, such as input and input-rate limits, $|u_i| \leq \overline{u}$ and $|\dot{u}_i| \leq \overline{\dot{u}}$. After synthesis of a feasible and achievable model set, the design task is to find control elements G and F, shown in Figure 1,

such that the reference to output transfer behaviour $Y_i/R = T_iF$ suitably approaches M_i for all plant cases, where

$$T_i = \frac{P_iG}{1 + P_iG} \tag{1}$$

is the complementary-sensitivity function for closed-loop plant i. The control elements should be sufficiently low order, for sake of implementation. Because time- and frequency-domain signals are only related via the integral over all frequencies (Fourier transform), the resulting closed-loop system may still violate the prescribed time-domain input constraints.[16]

2.2 | Reference model design

The reference model design is not the focus of this paper and will only be touched upon briefly here. For sake of simplicity, we use an all-pole reference model structure, with plant dependent dead time. The order of reference model M_i is chosen to be two greater than that of the corresponding P_i. This is to ensure that the operation $sU_i/R = sM_i/P_i$ is strictly proper (for plant input-rate consideration). Any NMP elements in the specific plant are included in the corresponding reference model to ensure that $U_i/R = M_i/P_i$ is a stable transfer function. For example, if P_1 is an all-pole plant of order m, and has a dead time of τ seconds, the corresponding reference model structure will be

$$M_1 = \frac{1}{1 + d_1s + d_2s^2 + \ \dots \ + d_{m+2}s^{m+2}}e^{-s\tau}, \tag{2}$$

where the coefficients, d_p, in (2) are the free parameters. An expected (potentially worst case) reference signal $R(s) = \mathcal{L}\{r(t)\}$, is used to generate the model response $Y_{m_i} = M_iR$, which is then converted into the corresponding time-domain signal y_{m_i}, using the inverse Laplace transform. Additionally, the time-domain reference model input, u_{m_i}, and input-rate, $\dot{u}_{m_i}$, can be found by taking the inverse Laplace transform of $(M_i/P_i)R$ and $(sM_i/P_i)R$, respectively. A simple cost function is then posed, which is a function of the time-domain reference tracking error, $e_i = r - y_{m_i}$. The time-domain constraints used are that of the plant input's limitations, namely, $|u_i| \leq \overline{u}$ and $|\dot{u}_i| \leq \overline{\dot{u}}$. The aforementioned information is placed in a constrained optimisation routine (*fmincon*[17]). This process is repeated for each plant in the plant set, and this generates a set of corresponding reference models. The resulting reference model set allows high performance tracking while also being achievable (in the context of the plant input capabilities).

2.3 | Controller synthesis

Consider the standard 2DOF control structure shown in Figure 1, where F is the prefilter, G is the feedback controller, **P** is the plant set, and H is the transfer function describing the sensor dynamics. For sake of simplicity, we will assume there is no significant measurement dynamics within the frequency range of interest ($H \approx 1$). If there were just two plants in the plant set, the control elements G and F could be solved for at equality ($F = M_1/T_1 = M_2/T_2$) to satisfy the model specifications exactly. For example, given $P_i \in \{P_1, P_2\}$ and $M_i \in \{M_1, M_2\}$, the control elements can be solved simultaneously as

$$F = \frac{M_1M_2(P_1 - P_2)}{M_1P_2 - M_2P_1}, \tag{3}$$

$$G = \frac{M_2P_1 - M_1P_2}{P_1P_2(M_1 - M_2)}. \tag{4}$$

Note that, if $M_1 = M_2$ and $P_1 \neq P_2$, G requires infinite gain to achieve the specifications with zero error, which is an obvious result for single model-error tracking problems. In addition, if $M_1 \neq M_2$ and $P_1 = P_2$, the specifications cannot be met for a single reference signal, as a single plant cannot have two different closed-loop transfer behaviours for a fixed control scheme.

When there are more than two plant-model specifications, each specification cannot be exactly met in general, owing to the fact that there are only two degrees of freedom in the control scheme. Instead, one would have to make a compromise across all plant-model combinations. This trade-off can be facilitated by using the method of model-error tracking specifications on a plant by plant basis. Similar to the work of Eitelberg,[7] the model-error tracking inequality for plant i is

$$|M_i - T_iF|\Big|_{\omega_d} = \left|M_i - \frac{P_iG}{1 + P_iG}F\right|\Big|_{\omega_d} \leq E|_{\omega_d} = E(\omega_d), \tag{5}$$

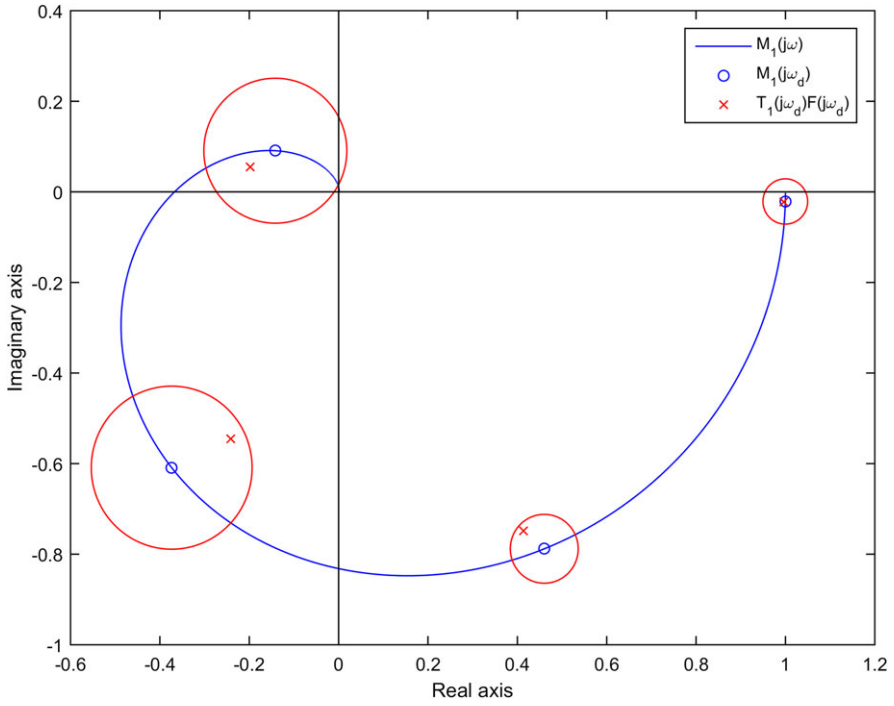

FIGURE 2 Arithmetic complex plane showing $M_1(j\omega)$, from (19) and Table 1, and the discrete model-error tracking requirements at $\omega_d \in \{0.1, 5, 10, 20\}$ rad/s. A valid solution of $T_1(j\omega_d)F(j\omega_d)$ will lie within the error circle, at the corresponding design frequency point ω_d [Colour figure can be viewed at wileyonlinelibrary.com]

where $E(\omega_d)$ is a user-defined model-tracking error radius (centred at $M_i(j\omega_d)$) and $\omega_d \in \{\mathbf{\Omega}\}, d \in \mathbb{Z}^+$. A valid solution at ω_d will therefore place $T_i(j\omega_d)F(j\omega_d)$ inside the corresponding error circle, as shown in Figure 2. With a sufficiently rich and appropriate set of discrete design frequency points, a continuous controller can then be designed, which satisfies the inequality across the discrete design space. The underlying assumption here is that the set of design frequency points, $\{\mathbf{\Omega}\}$, sufficiently covers the bandwidth of interest, in terms of the reference model set to be tracked. Note that the fundamental departure from the work of Eitelberg[7] is the existence of a bespoke reference model specification for each plant case, as opposed to a single reference model covering the entire plant set. Equation (5) is a function of both G and F, which makes the bandwidth trade-off between the control elements nontrivial. Conventionally, one might choose an appropriate nominal plant P_0, and fix the prefilter as $F_0 = M_0/T_0 = M_0(1 + P_0G)/(P_0G)$. This however has the effect of coupling the design of G to the choice of P_0, which can introduce unnecessary conservatism in the resulting controller solution space.[8] To avoid this, we instead build on the work of Elso et al,[10] as follows. Assuming $G(j\omega_d)$ in (5) were known, we require $F(j\omega_d) \in \mathbb{S}_{F_i(j\omega_d)}$, where $\mathbb{S}_{F_i(j\omega_d)}$ is the local solution space of $F(j\omega_d)$ for plant case i, which satisfies (5). $\mathbb{S}_{F_i(j\omega_d)}$ describes a disc, centred at $M_i(j\omega_d)/T_i(j\omega_d)$, with a radius of $E(\omega_d)/|T_i(j\omega_d)|$,

$$|M_i/T_i - F|\Big|_{\omega_d} \leq \frac{E}{|T_i|}\Big|_{\omega_d}. \tag{6}$$

The existence of a global solution space of $F(j\omega_d)$, namely, $\mathbb{S}_{F(j\omega_d)}$, requires a non-empty intersection across all local solution spaces of $F(j\omega_d)$,

$$\mathbb{S}_{F(j\omega_d)} = \cap_{i=1}^{m} \mathbb{S}_{F_i(j\omega_d)}. \tag{7}$$

With reference to Figure 3, this means that the distance between the centres of the solution spaces, $\mathbb{S}_{F_i(j\omega_d)}$ and $\mathbb{S}_{F_k(j\omega_d)}$, must be smaller than or equal to the sum of their respective radii, for all plant cases,

$$|M_i/T_i - M_k/T_k|\Big|_{\omega_d} \leq E\left(\frac{1}{|T_i|} + \frac{1}{|T_k|}\right)\Big|_{\omega_d}, \forall i, k, \quad i \neq k. \tag{8}$$

Note that the model-tracking error radius in (8) is common between plant i and k. This facilitates equal model-tracking performance across all plants in the plant set. Equation (8) can be written as a function of design variable $G(j\omega_d)$,

$$|M_iP_k(1 + P_iG) - M_kP_i(1 + P_kG)|\big|_{\omega_d} \leq E\,(|P_k(1 + P_iG)| + |P_i(1 + P_kG)|)\big|_{\omega_d}, \forall i, k, \quad i \neq k. \tag{9}$$

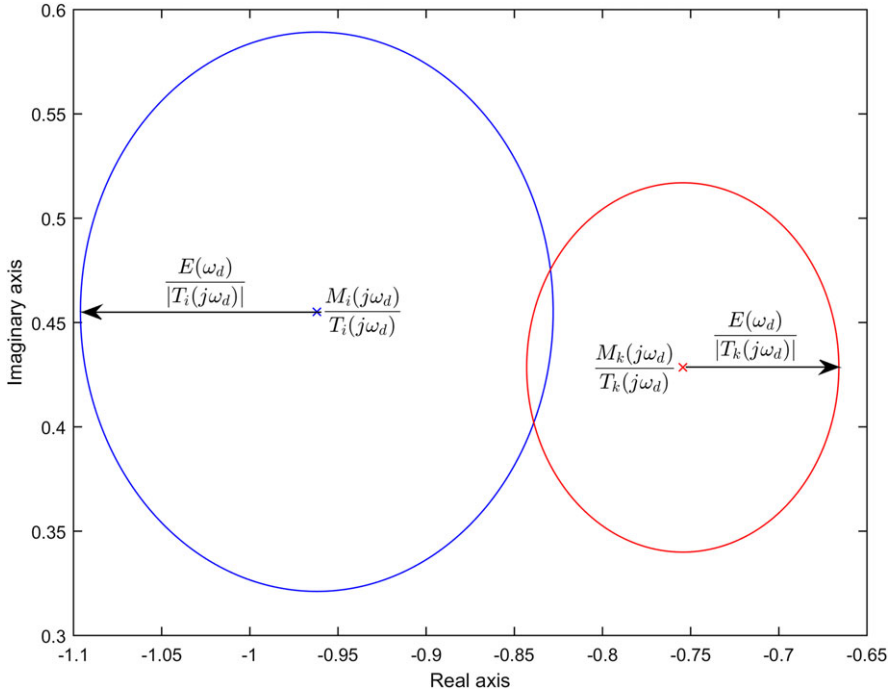

FIGURE 3 Arithmetic complex plane showing local solution spaces $\mathbb{S}_{F_i(j\omega_d)}$ (blue) and $\mathbb{S}_{F_k(j\omega_d)}$ (red). The intersection of the two local solution spaces describes the region where a potential solution, $F_{ik}(j\omega_d)$, can simultaneously satisfy both conditions [Colour figure can be viewed at wileyonlinelibrary.com]

Equation (9) is solely a function of $G(j\omega_d)$, and if satisfied for all plant combinations, guarantees the existence of a non-empty global solution space for $F(j\omega_d)$. Note that, if $M_i(j\omega_d) = M_k(j\omega_d)$ in (9), the aforementioned inequality matches the result from the work of Elso et al.[10] With reference to (8) and (9), the introduction of the per-plant models means that the existence of $\mathbb{S}_{F(j\omega_d)}$ may not be guaranteed as $|G(j\omega_d)| \to \infty$ (if $|M_i(j\omega_d) - M_k(j\omega_d)| > 2E(\omega_d)$, for any one $\{i, k\}$ combination). Instead, there will be unique phase-gain regions of G for the particular plant combination, which will minimise the tracking error. The feedback controller therefore does not perform its traditional role of uniformly reducing closed-loop uncertainty across the plant set, but rather attempts to correctly position each plant's complementary-sensitivity function to improve the overall plant set's model-tracking behaviour.

Equation (9) requires some manipulation to find the solution space $\mathbb{S}_{G_{ik}(j\omega_d)}$. This is done by first converting each element of the inequality in (9) to its magnitude-phase form, eg, $P_k(j\omega_d) = |P_k|e^{j\theta_k}|_{\omega_d}$, and $G(j\omega_d) = |G|e^{j\psi}|_{\omega_d}$. The controller phase angle, ψ, is swept across its full range (0° to −360°), such that $|G(j\omega_d)|$ is the only unknown in the equation, for a given ω_d. At each controller phase, (9) can be represented as

$$|z_1| \leq |z_2| + |z_3|, \tag{10}$$

where z_p is a complex number, and the dependence on $|G(j\omega_d)|$, ψ, and ω_d, is omitted for sake of clarity. Given that $|z_p| = \sqrt{z_p z_p^*}$, squaring both sides will yield

$$z_1 z_1^* \leq z_2 z_2^* + 2\sqrt{z_2 z_2^* z_3 z_3^*} + z_3 z_3^*. \tag{11}$$

Next, leaving only the square rooted term on the right-hand side, and squaring again gives

$$\left(z_1 z_1^* - z_2 z_2^* - z_3 z_3^*\right)^2 \leq 4 z_2 z_2^* z_3 z_3^*. \tag{12}$$

Finally, subtracting the left-hand side from the right-hand side in (11) gives the quartic polynomial inequality[18] in $|G(j\omega_d)|$,

$$a_1(\omega_d, \psi)|G(j\omega_d)|^4 + a_2(\omega_d, \psi)|G(j\omega_d)|^3 + a_3(\omega_d, \psi)|G(j\omega_d)|^2 + a_4(\omega_d, \psi)|G(j\omega_d)| + a_5(\omega_d, \psi) \geq 0, \tag{13}$$

where the coefficients in (13) are functions of the design frequency point and controller phase angle (after evaluating all the plant and model elements). If $M_i(j\omega_d) = M_k(j\omega_d)$, as in the work of Elso et al,[10] (13) reduces to a quadratic inequality. The four roots of (13) can be obtained using standard root-finding methods. Note that because of the squaring operations,

there can be up to two valid roots, which correspond to the original inequality of (9). These valid roots will then serve as upper or lower bounds on the solution space of $|G(j\omega_d)|$, for a particular ψ, depending on the profile of the quartic polynomial. This means that there can be up to two bounded regions where $|G(j\omega_d)|$ satisfies (9).

After sweeping across the entire controller phase range, one obtains the local solution space of $\mathbb{S}_{G_{ik}(j\omega_d)}$. The global solution space (if it exists), for a particular design frequency point, follows as the non-empty intersection across all plant combinations

$$\mathbb{S}_{G(j\omega_d)} = \cap_{i=1,k=1}^{m,m} \mathbb{S}_{G_{ik}(j\omega_d)}. \tag{14}$$

Note that interchanging index i and k in (9) does not affect the inequality. Additionally, the case of $i = k$ satisfies (9) for all values of $G(j\omega_d)$. This means that there will be $\binom{m}{2} = m(m-1)/2$ unique plant combinations for a particular design frequency point. Once $\mathbb{S}_{G(j\omega_d)}$ is obtained for all frequency points, it can be visualised in the log-polar plane, for shaping the feedback controller. The underlying requirement is that $G(j\omega_d) \in \mathbb{S}_{G(j\omega_d)}$, for each design frequency point. Depending on the specification of $E(\omega_d)$, this may not be possible for all plant combinations. In addition, continuous G needs to satisfy Bode integral relations (ie, be physically realisable). If $E(\omega_d)$ is not a user specification, but rather a free design parameter, one could instead use a level set of error radii to provide insight with regard to what is achievable.[19] Design frequency point ω_d will then have a solution space, $\mathbb{S}_{G(j\omega_d,w)}$, corresponding to the chosen error radii $E_w(\omega_d) \in \{\mathbf{E}(\omega_d)\}$, where $w \in \mathbb{Z}^+$. The solution space for a particular $E_w(\omega_d)$ will be a subset of the solution space for any larger error radius, meaning that the admissible design regions will expand monotonically as the error radius is increased. Additionally, the relative expansion of the bounds, for linearly increasing error radii, is related to the gradient of the tracking tolerance, and corresponds to the sensitivity of the error tracking with respect to changes in the control element of interest, at the particular design frequency point. This gives the designer valuable insight into "cost-effective" loop shaping and design frequency performance trade-offs. The relationship between the controller complexity and frequency-based model tracking performance is also made transparent.

Once the feedback element has been chosen, the prefilter can be designed. With $\mathbf{T}$ fixed, (5) describes a linear fractional mapping on $F(j\omega_d)$, which can be resolved to find $\mathbb{S}_{F_i(j\omega_d)}$ at each design frequency point.[20] The global solution space of $F(j\omega_d)$ can then be found using (7). The per-frequency solution spaces can be represented in the log-polar plane by comparing the logarithmic gain and phase requirements of $F(j\omega_d)$. With reference to (8) and Figure 3, the choice of G (and by association, $\mathbf{T}$) will affect the shape and size of $\mathbb{S}_{F(j\omega_d)}$. One could perform the prefilter bound generation using the same per-frequency error sets from the feedback design stage. However, the additional knowledge gained from fixing G means that it may be more informative to reassess the achievable error tolerances. Referring to (9), the minimum achievable model-tracking error at design frequency point ω_d is

$$E_{0ik}(\omega_d) = \left.\frac{|M_iP_k(1+P_iG) - M_kP_i(1+P_kG)|}{|P_k(1+P_iG)| + |P_i(1+P_kG)|}\right|_{\omega_d}, \tag{15}$$

for plant pairs i and k. By evaluating (15) for all plant combinations, one can find the extremum, which corresponds to the minimum tracking error achievable across all plant cases

$$E_0(\omega_d) = \max\{E_{0ik}(\omega_d)\}, \forall\ i,k, \quad i \neq k. \tag{16}$$

This can then be used as a starting point for growing the error contours for use in the prefilter design. Although not directly specified, the original per-plant model-error tracking specifications nonarbitrarily bound the reference to plant input transfer behaviour, with respect to the corresponding model behaviour. Consulting the original specifications in (5), dividing both sides by $|P_i(j\omega_d)|$ gives

$$\left.\left|\frac{M_i}{P_i} - \frac{GF}{1+P_iG}\right|\right|_{\omega_d} \leq \frac{E(\omega_d)}{|P_i(j\omega_d)|}, \tag{17}$$

where M_i/P_i is the ideal reference to plant input behaviour (from the model optimisation stage), and $U_i/R = GF/(1+P_iG)$ is the closed-loop reference to plant input behaviour. It follows that U_i/R will approach the ideal reference to plant input behaviour as the model-tracking error approaches zero. In stark contrast, if there were instead a single nominal reference model, U_i/R would approach M_0/P_i, which may be physically infeasible for low gain plants (in a signal constraint sense). It is worth emphasizing that this frequency-domain method is not a solution to the time-domain saturation problem. However, the inclusion of physically realistic reference models (using constrained optimisation), gives the designer a better handle on the problem.

TABLE 1 Table of plant parameters and corresponding optimised model parameters

i	1	2	3	4	5	6	7	8
k_i	10	10	30	30	10	10	30	30
α_i	25	35	25	35	25	35	25	35
τ_i	0	0	0	0	0.02	0.02	0.02	0.02
a_i	7.72×10^{-6}	6.21×10^{-6}	1.95×10^{-6}	1.52×10^{-6}	7.72×10^{-6}	6.21×10^{-6}	1.95×10^{-6}	1.52×10^{-6}
b_i	9.32×10^{-4}	7.65×10^{-4}	2.61×10^{-4}	2.07×10^{-4}	9.32×10^{-4}	7.65×10^{-4}	2.61×10^{-4}	2.07×10^{-4}
c_i	1.81×10^{-2}	1.63×10^{-2}	7.87×10^{-3}	6.75×10^{-3}	1.81×10^{-2}	1.63×10^{-2}	7.87×10^{-3}	6.75×10^{-3}
d_i	0.21	0.20	0.14	0.13	0.21	0.20	0.14	0.13

3 | WORKED EXAMPLE

Consider the simple plant set

$$\mathbf{P} = \frac{\mathbf{k}}{s(1 + s/\boldsymbol{\alpha})} e^{-s\boldsymbol{\tau}}, \tag{18}$$

where the plant has input magnitude and rate constraints of $|u(t)| \leq \overline{u} = 0.6$ and $|\dot{u}(t)| \leq \overline{\dot{u}} = 5$, respectively. For sake of simplicity, the expected reference signal is the unit step, $R(s) = 1/s$. With reference to Section 2.2, the associated model is chosen to be a 4^{th} order all-pole filter, with a pure delay term matching that of the particular plant

$$\mathbf{M} = \frac{1}{\mathbf{a}s^4 + \mathbf{b}s^3 + \mathbf{c}s^2 + \mathbf{d}s + 1} e^{-s\boldsymbol{\tau}}. \tag{19}$$

The plant and reference model parameters from (8) and (9) are detailed in Table 1.

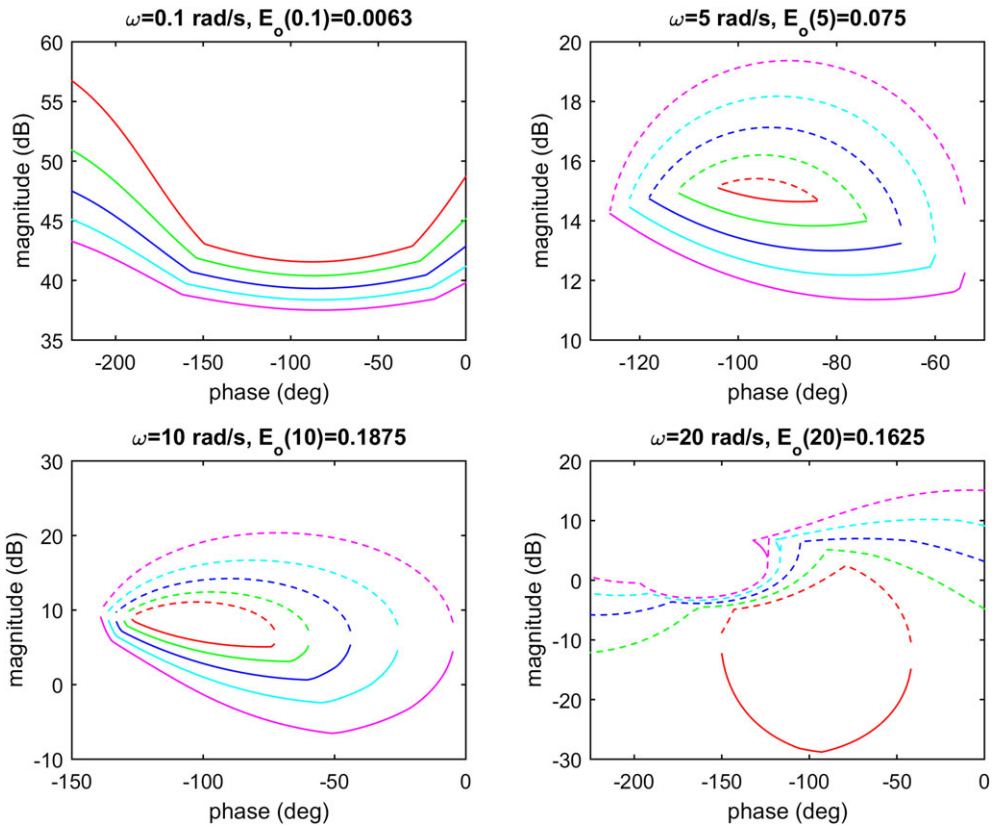

FIGURE 4 Level set of solution spaces for $G(j\omega)$ at four discrete design frequency points. Solid line corresponds to "stay-above" bound, and dotted line corresponds to "stay-below" bound, for $\omega_d \in \{0.1, 5, 10, 20\}$ rad/s. The error radii at design frequency point ω_d is generated by scaling $E_0(\omega_d)$ by [1,1.2,1.4,1.6,1.8] [Colour figure can be viewed at wileyonlinelibrary.com]

With the model set fully defined, the process of designing G and F can begin. It is worth mentioning that traditionally selecting a nominal prefilter of $F_0 = M_0/T_0$ would be problematic here, as the variable plant delay in (18) makes the choice of a "good" nominal plant very difficult. Because there are no hard specifications on the allowable model-tracking error, it is treated as a free parameter, and gauged on a per-frequency basis. As previously mentioned, this is done by treating the model-tracking error as a level set, which results in contoured solution spaces. Because G is not yet known, the minimum achievable error tracking radius $E_0(\omega_d)$, is approximated by resolving (9) for monotonically increasing $E(\omega_d)$ values, starting from zero. The first value of $E(\omega_d)$, which yields a non-empty solution space for all plant combinations, is then treated as the minimum achievable error tracking radius for the particular discrete design frequency point. This minimum can then be linearly scaled (for example) to generate a level set of achievable error radii. Figure 4 shows a set of global solution spaces of G, for a few design frequency points. As previously mentioned, these per-frequency bounds describe a monotonically expanding design region or "contour map," which collectively indicates what level of model-error tracking is achievable across all discrete frequencies and plant cases. Note that, even if a certain error bound at ω_d is satisfied by some $G(j\omega_d)$, it may be infeasible, depending on the collective bound requirements on continuous G, as the control elements must obey the Bode gain-phase constraints. This is also true for the design of F. An appropriate subset of the bounds shown in Figure 4 can be used to design G.

For sake of stability robustness, a bound is placed on the closed-loop sensitivity of

$$|S_i(j\omega_d)|_{db} = \left|\frac{1}{1 + P_i(j\omega_d)G(j\omega_d)}\right|_{db} \leq 6\,\text{db}, \forall \omega_d \in \{\mathbf{\Omega}\}, P_i \in \{\mathbf{P}\}. \tag{20}$$

Additionally, high-frequency noise attenuation is addressed by requiring G to be strictly proper. The combination of the sensitivity bounds and model-tracking bounds are shown in Figure 5.

In both cases, the bounds on G are shifted and scaled by the same arbitrarily chosen $P_0 = P_4$ to show the nominal loop transfer behaviour on a Nichols chart. Although this does not affect the admissible design regions of G, it helps with visualisation for designers who are used to the Nichols chart. With reference to Figure 5, there are strict gain and phase constraints in the frequency band of 5 rad/s to 15 rad/s (near the gain-phase cross-over region). In contrast, the high- and low-frequency design requirements have more design freedom, as G has minimal impact at high frequencies, and is not

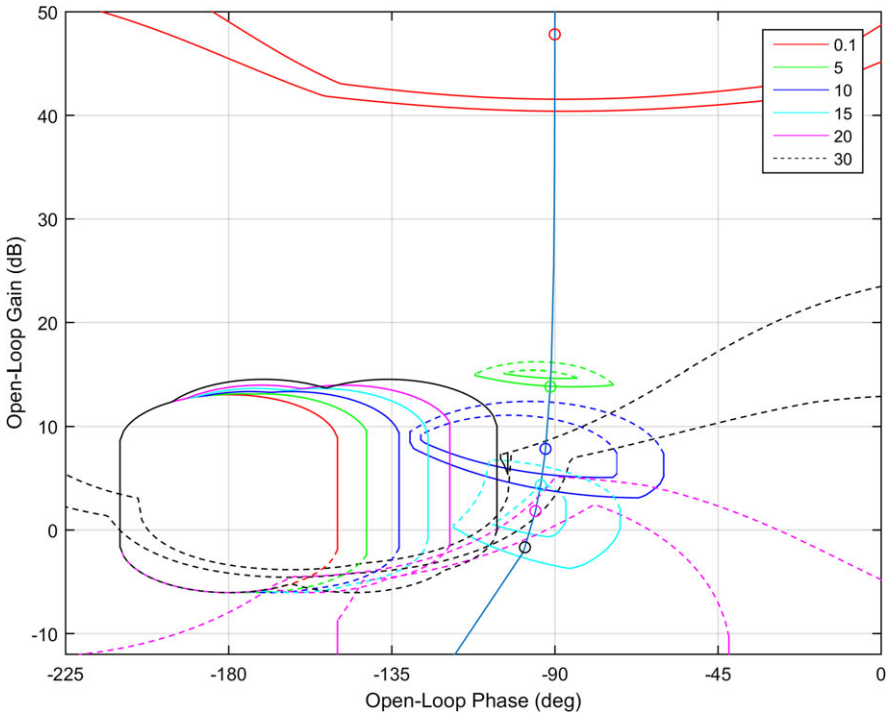

FIGURE 5 Nichols chart of $|L_0(j\omega)|_{db}$ versus $arg\{L_0(j\omega)\}$, showing sensitivity and model-tracking bounds, on nominal loop $L_0(j\omega) = P_0(j\omega)G(j\omega)$, for $\omega_d \in \{0.1, 5, 10, 15, 20, 30\}$ rad/s. Two model-tracking solution spaces are shown at each discrete design frequency point, using $E_w(\omega_d) \in \{E_0(\omega_d), 1.2E_0(\omega_d)\}$ as the error specification. The resulting nominal loop transfer behaviour, after designing G, is also shown [Colour figure can be viewed at wileyonlinelibrary.com]

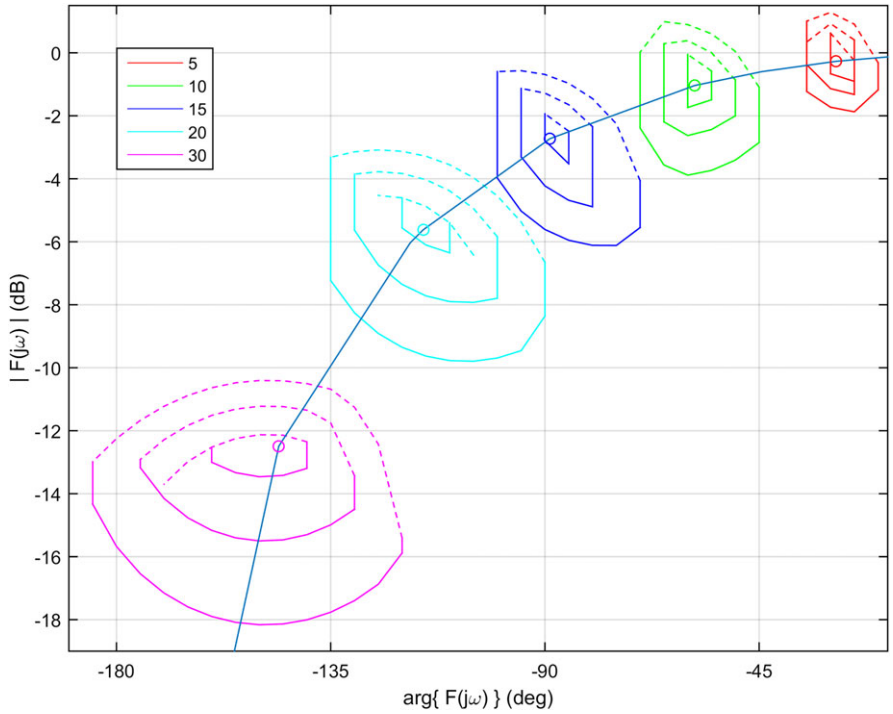

FIGURE 6 Log-polar plot of $|F(j\omega)|_{db}$ versus $arg\{F(j\omega)\}$, showing multiple global solution spaces of $F(j\omega_d)$, using three error specifications, for $\omega_d \in \{5, 10, 15, 20, 30\}$ rad/s. The designed prefilter, F, is also shown [Colour figure can be viewed at wileyonlinelibrary.com]

required at low frequencies (for type 1 plants). With the secondary design goal of sufficiently low-order control design in mind, the resulting controller is chosen to be

$$G = 0.82\frac{(1 + s/33.94)}{(1 + s/529.5)(1 + s/287.9)}. \tag{21}$$

The feedback controller is second order, and has the required high-frequency roll-off of −20 db/dec. Note that the model-error tracking in Figure 5 could be improved, but at the cost of a more complex feedback controller. The trade-off however is transparent when using the level set of error radii. Following the design of G, the achievable error tolerances are re-evaluated based on (15). The design of F is then formulated using the original per-plant model-error tracking inequality of (5). Figure 6 shows the per-frequency global solution spaces of $F(j\omega_d)$, visualised in the log-polar plane. A sufficiently low-order prefilter, which suitably reduces the frequency-based error tolerances, is

$$F = \frac{(1 + s/35.36)(1 + s/387.5)}{(1 + s/15.29)(1 + 2(0.62)/19.05s + s^2/19.05^2)}. \tag{22}$$

Again, it should be noted that by using a level set of error radii, one can easily trade controller complexity with error tracking performance. Additionally, the Bode gain-phase requirements means that the smallest error bounds may not be achievable across all discrete design frequency points. Although the reference models are designed to satisfy the input constraints, because nonzero tracking error is allowed, time-domain simulation is required to check the input signal levels (and rates). The set of output responses, $\mathbf{y}(t)$, and corresponding model responses, $\mathbf{y}_m(t)$, is shown in Figure 7. With reference to Figure 7, the output step responses are located near their associated model responses. In fact, there appears to be two major groupings, which correspond to the high and low gain plants, respectively. The model-matching ability of the uncertain system is fundamentally limited by the "agreement" of the individual reference models, with respect to the plant set. For example, if one were to initially fix $G = G_0$ and $F = F_0$, and then use the resulting closed-loop performance as the reference model, the 2DOF controller solution space would contain a single solution of $G = G_0$ and $F = F_0$, which yields exact model-matching across the plant set (perfect "agreement"). The closed-loop input and input-rate responses are shown in Figure 8. The two time-domain responses of Figures 7 and 8 reaffirm that each closed-loop plant can operate near its corresponding reference model, without requiring exotic input and input-rate commands.

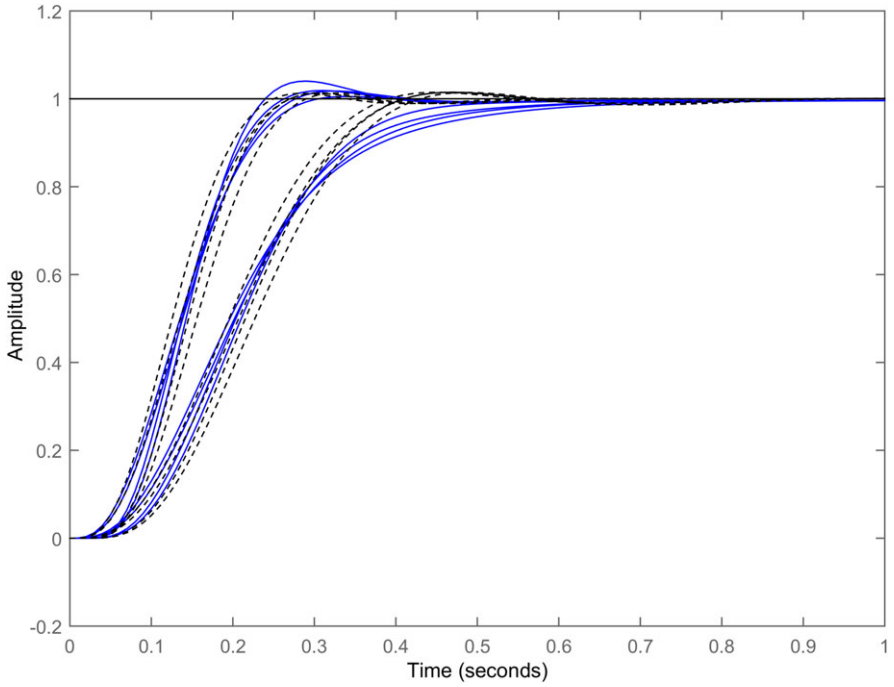

FIGURE 7 Step response of closed-loop plant set (blue) and corresponding model set (black), for a reference signal of $r(s) = 1/s$, applied at $t = 0$ seconds [Colour figure can be viewed at wileyonlinelibrary.com]

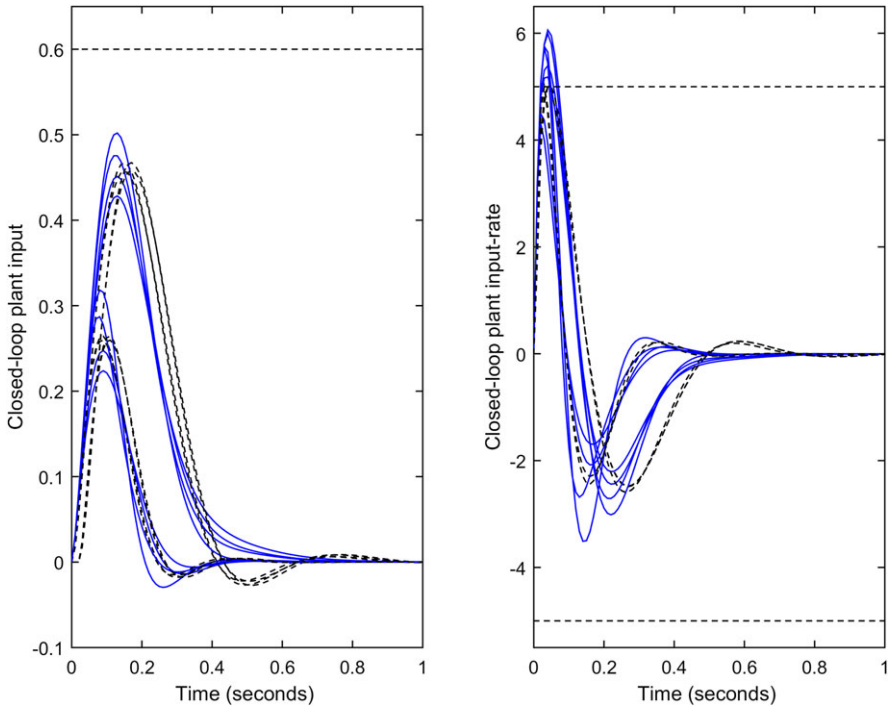

FIGURE 8 Closed-loop plant input response (left) and plant input-rate response (right) for plant set, shown in blue. The corresponding reference model responses are also shown (dotted lines) [Colour figure can be viewed at wileyonlinelibrary.com]

4 | CONCLUSION

This paper has presented a new approach to designing a robust controller for an uncertain plant set. In particular, it was shown that by applying bespoke tracking specifications to each plant case, based on that plant's capability, the plant set could achieve improved, realistic overall performance. Additionally, making use of error radii level sets, the

frequency-based performance versus controller complexity trade-offs were made transparent. The method was illustrated using a simple problem, which yielded the expected per-plant model following, given the large plant set uncertainty. This design methodology is particularly useful for discrete plant sets with fundamentally different gain-phase profiles.

ORCID

Arnold Pretorius https://orcid.org/0000-0002-1940-588X
Edward Boje https://orcid.org/0000-0003-2733-3537

REFERENCES

1. Horowitz I. Quantitative feedback theory. *IEE Proc D (Control Theory Appl)*. 1982;129(6):215-226.
2. Horowitz I. Invited paper survey of quantitative feedback theory (QFT). *Int J Control*. 1991;53(2):255-291.
3. Yaniv O. *Quantitative Feedback Design of Linear and Nonlinear Control Systems*. Vol. 509. New York, NY: Springer Science and Business Media; 2013.
4. Houpis CH, Rasmussen SJ. *Quantitative Feedback Theory: Fundamentals and Applications*. New York, NY: Marcel Dekker, Inc; 1999.
5. Bailey FN, Hui CH. CACSD tools for loop gain-phase shaping design of SISO robust controllers. In: 1998 IEEE Control Systems Society Workshop on Computer-aided Control System Design; 1989; Tampa, FL.
6. Moreno JC, Baños A, Berenguel M. The design of QFT robust compensators with magnitude and phase specifications. *Math Probl Eng*. 2010;2010. Article ID 105143.
7. Eitelberg E. Quantitative feedback design for tracking error tolerance. *Automatica*. 2000;36(2):319-326.
8. Elso J, Gil-Martínez M, Garcia-Sanz M. Nonconservative QFT bounds for tracking error specifications. *Int J Robust Nonlinear Control*. 2012;22(18):2014-2025.
9. Boje E. Pre-filter design for tracking error specifications in QFT. *Int J Robust Nonlinear Control: IFAC-Affil J*. 2003;13(7):637-642.
10. Elso J, Gil-Martínez M, García-Sanz M. Quantitative feedback–feedforward control for model matching and disturbance rejection. *IET Control Theory Appl*. 2013;7(6):894-900.
11. Franchek MA, Herman PA. Direct connection between time-domain performance and frequency-domain characteristics. *Int J Robust Nonlinear Control: IFAC-Affil J*. 1998;8(12):1021-1042.
12. Horowitz I. A synthesis theory for a class of saturating systems. *Int J Control*. 1983;38(1):169-187.
13. Wu W, Jayasuriya S. A new QFT design methodology for feedback systems under input saturation. *J Dyn Syst Meas Control*. 2001;123(2):225-232.
14. Pritchard CJ, Wigdorowitz B. On the determination of time-domain signal levels at the specification stage in quantitative feedback theory controller synthesis. *Int J Control*. 1997;66(2):329-348.
15. Moreno JC, Guzmán J, Baños A, Berenguel M. The input amplitude saturation problem in QFT: a survey. *Annu Rev Control*. 2011;35(1):34-55.
16. Hippe P, Stahl H. Note on the relation between pole-zero location and input-output behaviour of SISO systems and its influence on controller design. *Int J Control*. 1987;45:1469-1477.
17. Matlab optimization toolbox; 2015.
18. Boje E. Algorithm for calculating MIMO QFT tracking bounds. *J Dyn Syst Meas Control*. 2004;126(3):697-699.
19. Boje E. Quantitative digital design of crossfeed and feedback controllers for the UH-60 black hawk helicopter. In: 1999 International Symposium on Quantitative Feedback Theory and Robust Frequency Domain Methods; 1999; Durban, South Africa.
20. Chait Y, Borghesani C, Zheng Y. Single-loop QFT design for robust performance in the presence of non-parametric uncertainties. *J Dyn Syst Meas Control*. 1995;117(3):420-425.

How to cite this article: Pretorius A, Boje E. Robust plant by plant control design using model-error tracking sets. *Int J Robust Nonlinear Control*. 2019;29:3330–3340. https://doi.org/10.1002/rnc.4553